Electronic Supplementary Material (ESI) for Sensors & Diagnostics.

Supporting information

Graphitic carbon nitride with Cu^{2+} and triazole groups co-doping for enhanced peroxidase-like activity and its application for glutathione detection

Xiaotao Liu, Xueyi Zheng, Chunqiu Xia, Liangqia Guo*

Ministry of Education Key Laboratory for Analytical Science of Food Safety and Biology, Fujian Provincial Key Laboratory of Analysis and Detection Technology for Food Safety, College of Chemistry, Fuzhou University, Fuzhou 350116, China.

Email: lqguo@fzu.edu.cn (L. Guo)

Characterization

Transmission electron microscopy (TEM) images were obtained by an FEI Tecnai G2F20 transmission electron microscope (FEI, USA). Dynamic light scattering data (DLS) were corrected by a Malvern Zetasizer Nano-2s laser particle size and zeta potential analyzer (Malvern, UK). X-ray diffraction (XRD) patterns were characterized by a Bruker D8 advance diffractometer with Cu Kα1 radiation (Bruker, German). Fourier transform infrared (FT-IR) spectra were recorded on a Nicolet 6700 FTIR spectrometer (Thermo, USA) using a KBr pellet. X-ray photoelectron spectroscopy (XPS) spectra were collected by a Thermo Scientific ESCALAB 250 (Thermo Fisher, USA) with an Al Kα source. Absorption spectrum of the solution was obtained on a Tecan Spark microplate reader (Tecan, Switzerland). Copper content in g-C_3N_4-Cu^{2+} NSs and g-C_3N_4-Cu^{2+} NSs was measured by an Agilent 7800 inductively coupled plasma mass spectrometer (ICP-MS) (Agilent, USA).

Cell culture and pretreatment of HeLa cells

HeLa cells were cultured in 1640 medium containing 10 % FBS, penicillin (100 UmL^{-1}) and streptomycin (100 mg mL^{-1}), and incubated at 37 °C in a humidified 5% CO_2 incubator. Every 48 h the medium was removed and HeLa cells were collected by brief trypsinization. To obtain the cell lysates, protein-removing reagent with 3 times volume of the cells was added to the suspended HeLa cells (~ 2.0×10^6), and the mixture was treated by freezing (in liquid nitrogen for 10 min) and thawing (in 37

ºC water bath for 5 min) for 3 cycles. The mixture was placed in ice bath for 10 min, and then was centrifuged at 12000 rpm for 10 min. The supernatant was collected and then diluted 400 times. The diluted supernatant was used for the detection of GSH.

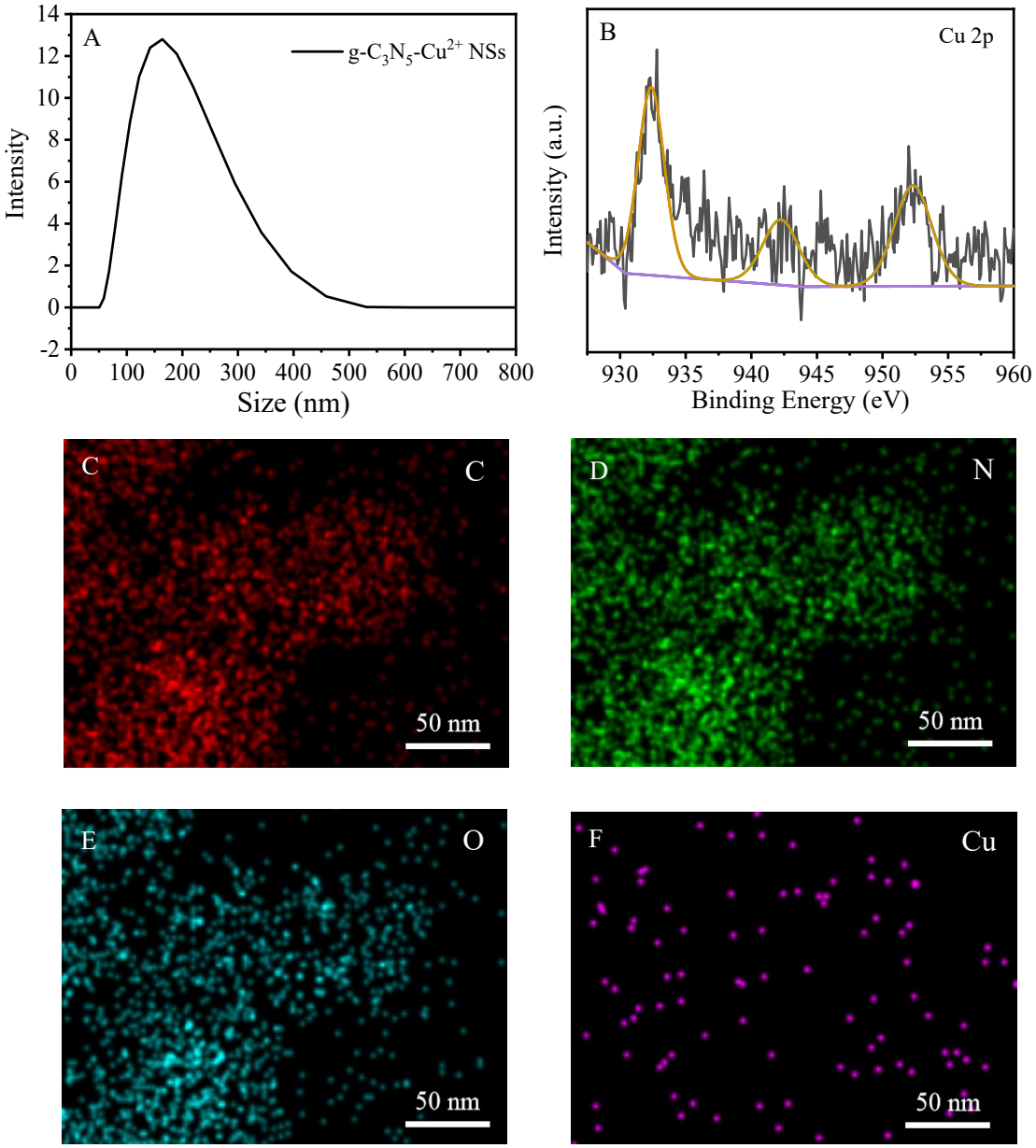

Figure S1. Particle size distribution (A), Cu 2p core-level XPS spectrum (B), energy-dispersive spectroscopy mapping (C-F) of g-C_3N_5-Cu^{2+} NSs.

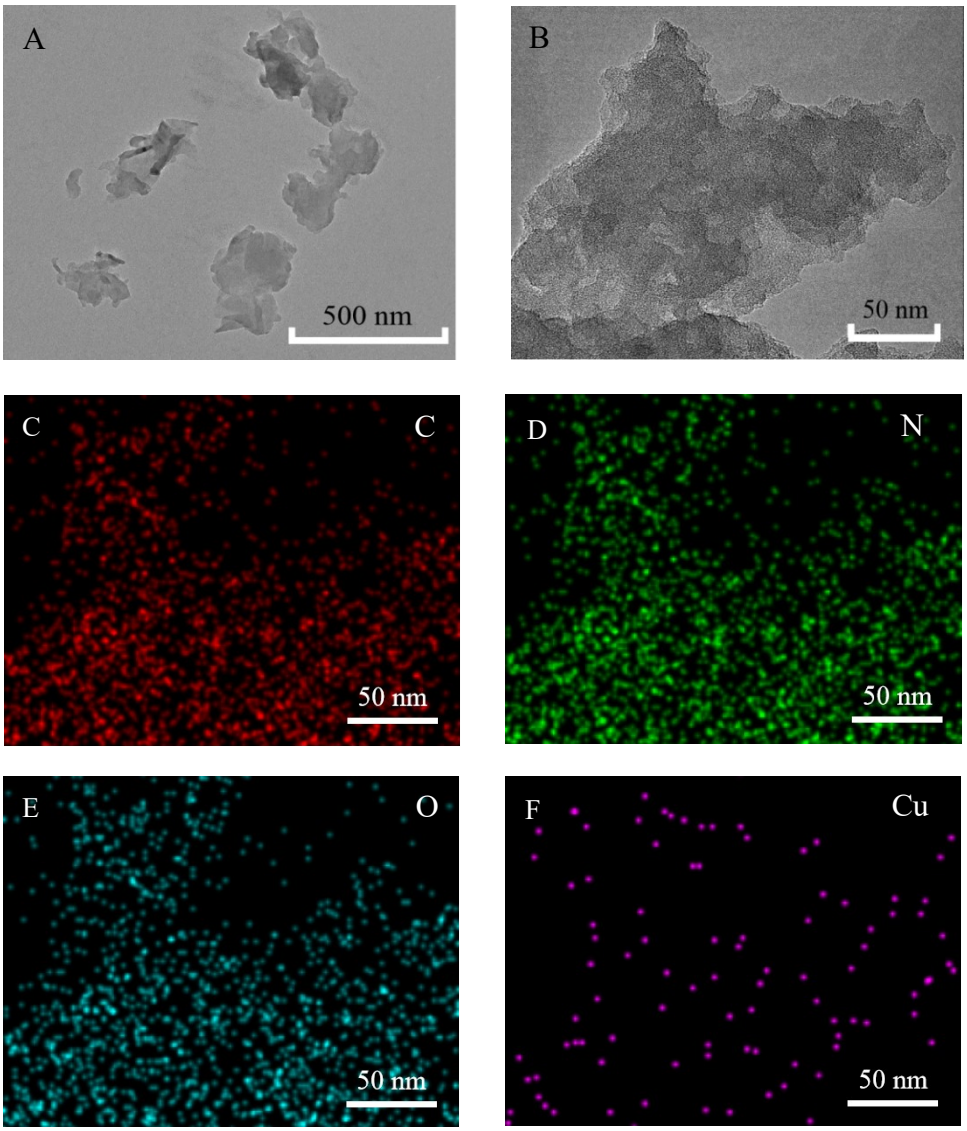

Figure S2. Characterization of g-C_3N_4-Cu^{2+}. TEM (A), high resolution TEM (B), energy-dispersive spectroscopy mapping (C-F).

g-C_3N_4-Cu^{2+} NSs show sheet-like structure with the lateral sizes ranged from dozens to about 300 nm (**Figure S2A-B**). The energy-dispersive spectroscopy mapping in **Figure S2C-F** further confirmed that the Cu^{2+} is well distributed in the frameworks of g-C_3N_4-Cu^{2+} NSs, and the mass of Cu^{2+} in g-C_3N_4-Cu^{2+} NSs is about 2.06 %, indicating the mass of Cu^{2+} in g-C_3N_4-Cu^{2+} NSs was higher than g-C_3N_5-Cu^{2+} NSs.

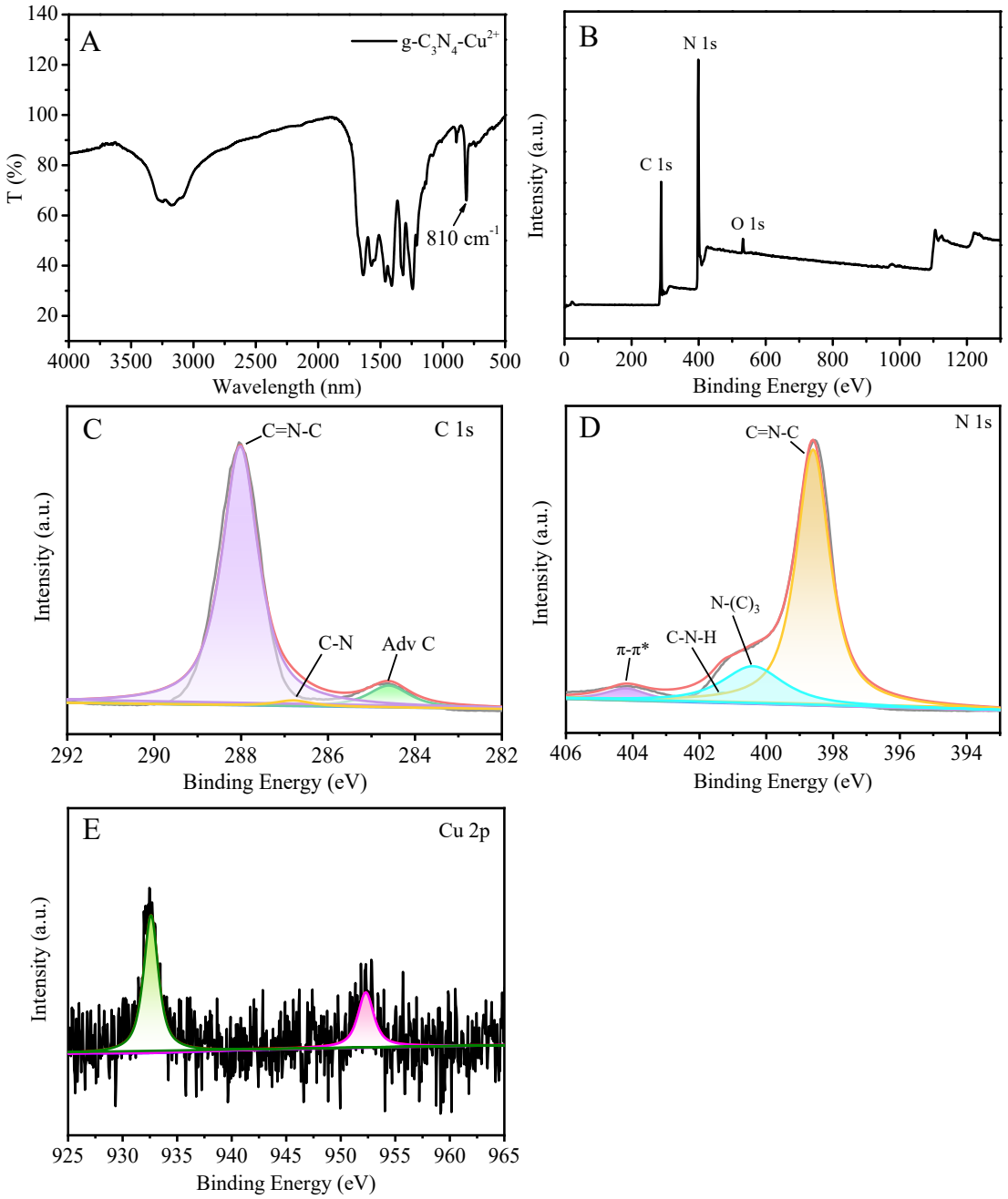

Figure S3. FT-IR (A), survey (B), C 1s (C), N 1s (D), Cu 2p (E) core-level XPS spectra of g-C_3N_4-Cu^{2+}.

A sharp absorption band at 810 cm^{-1} is belonged to the characteristic breathing mode of (tri-s-)triazine ring (**Figure S3A**). It is worthy to mention there is no characteristic absorption band of triazole groups at 1425 cm^{-1}, which is remarkably

different from g-C_3N_5-Cu^{2+} NSs. The XPS spectrum (**Figure S3B-E**) of g-C_3N_4-Cu^{2+} NSs is similar to that of g-C_3N_5-Cu^{2+} NSs. The C 1s core-level spectrum (**Figure S3C**) can be deconvolved into three components with binding energies (BEs) at 284.6, 286.6 and 293.6 eV, corresponding to adventitious carbon (Adv. C), sp^3-bound carbon (C-N), the carbon atoms bonded with three neighbor nitrogen atoms (N=C-N_2). The N 1s core-level XPS spectrum (**Figure S3D**) can be deconvolved into four components with the BEs at 398.8, 400.7, 401.3 and 404.2 eV, belonging to pyridine nitrogen (C-N=C), pyrrole nitrogen (N-$(C)_3$), amino group (C-NH_2) and the π electron delocalization in carbon nitride heterocycles (π-excitations). In the Cu 2p core-level XPS spectrum (**Figure 3E**), there are two strong peaks at 932.4 and 952.2 eV, corresponding to Cu $2p_{3/2}$ and Cu $2p_{1/2}$, which are characteristic peaks of Cu^{2+}.[S1]

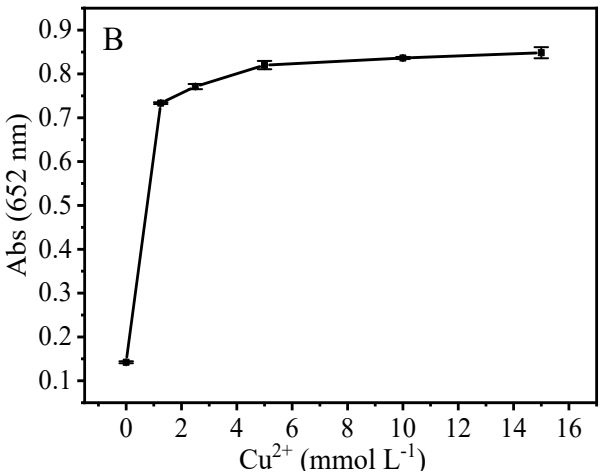

Figure S4. Effect of Cu^{2+} concentration on absorbance of the mixture solution of g-C_3N_5-Cu^{2+} NSs, TMB and H_2O_2. Conditions: Tris-HCl (pH 3, 50 mmol L^{-1}), g-C_3N_5-Cu^{2+} NSs (0.1 mg mL^{-1}), TMB (1.2 mmol L^{-1}), H_2O_2 (80 μmol L^{-1}). Reaction temperature was 37 °C, incubating time was 30 min. Insert of A are the photos of corresponding mixture solution.

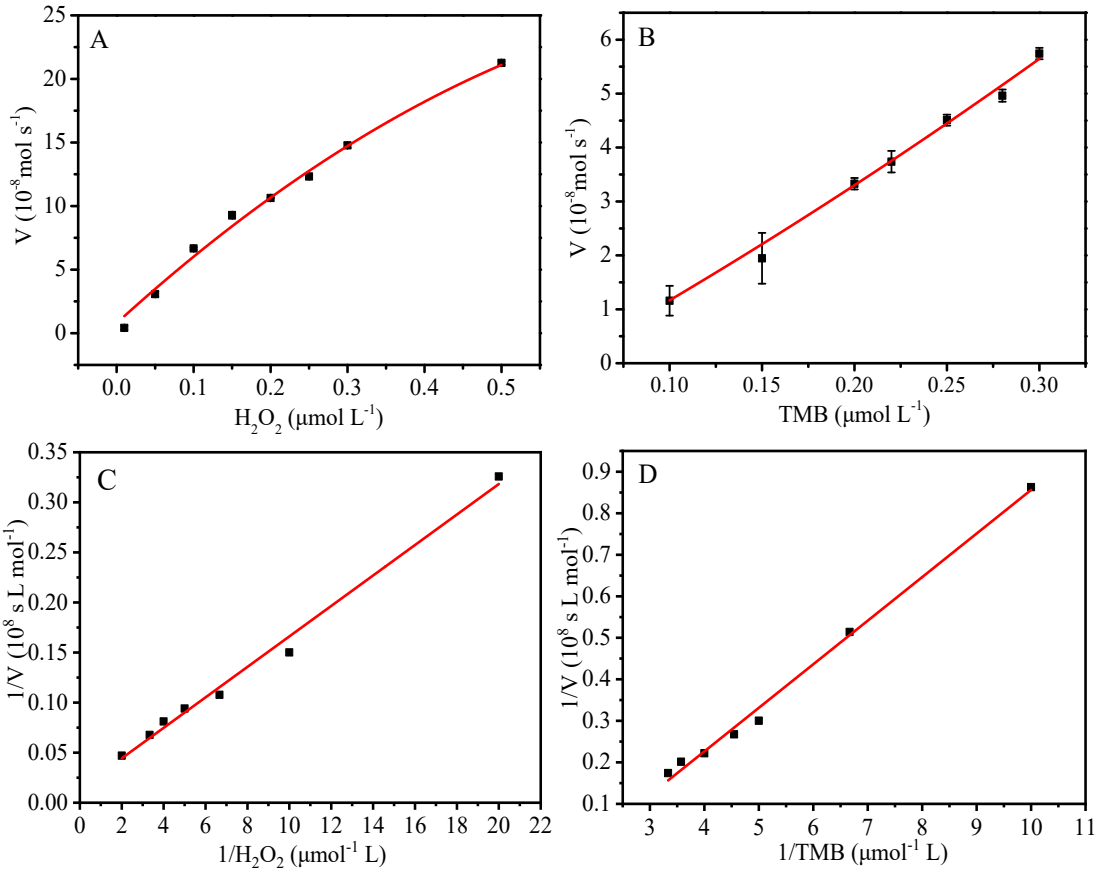

Figure S5. The steady-state kinetic and catalytic mechanism of g-C_3N_5-Cu^{2+} NSs. The velocity (v) of the reaction was measured by using g-C_3N_5-Cu^{2+} NSs (0.1 mg mL^{-1}) in Tris-HCl buffer (20 mmol L^{-1}, pH 6.5) incubated at 50 °C for 30 min. The error bars represented the standard error derived from three repeated measurements. TMB concentration was 1.0 mmol L^{-1}, and H_2O_2 concentration was varied (A). H_2O_2 concentration was 80 μmol L^{-1}, and TMB concentration was varied (B). Double reciprocal plots of catalytic activity of g-C_3N_5-Cu^{2+} NSs with the concentration of one substrate (TMB or H_2O_2) fixed and the other varied (C, D).

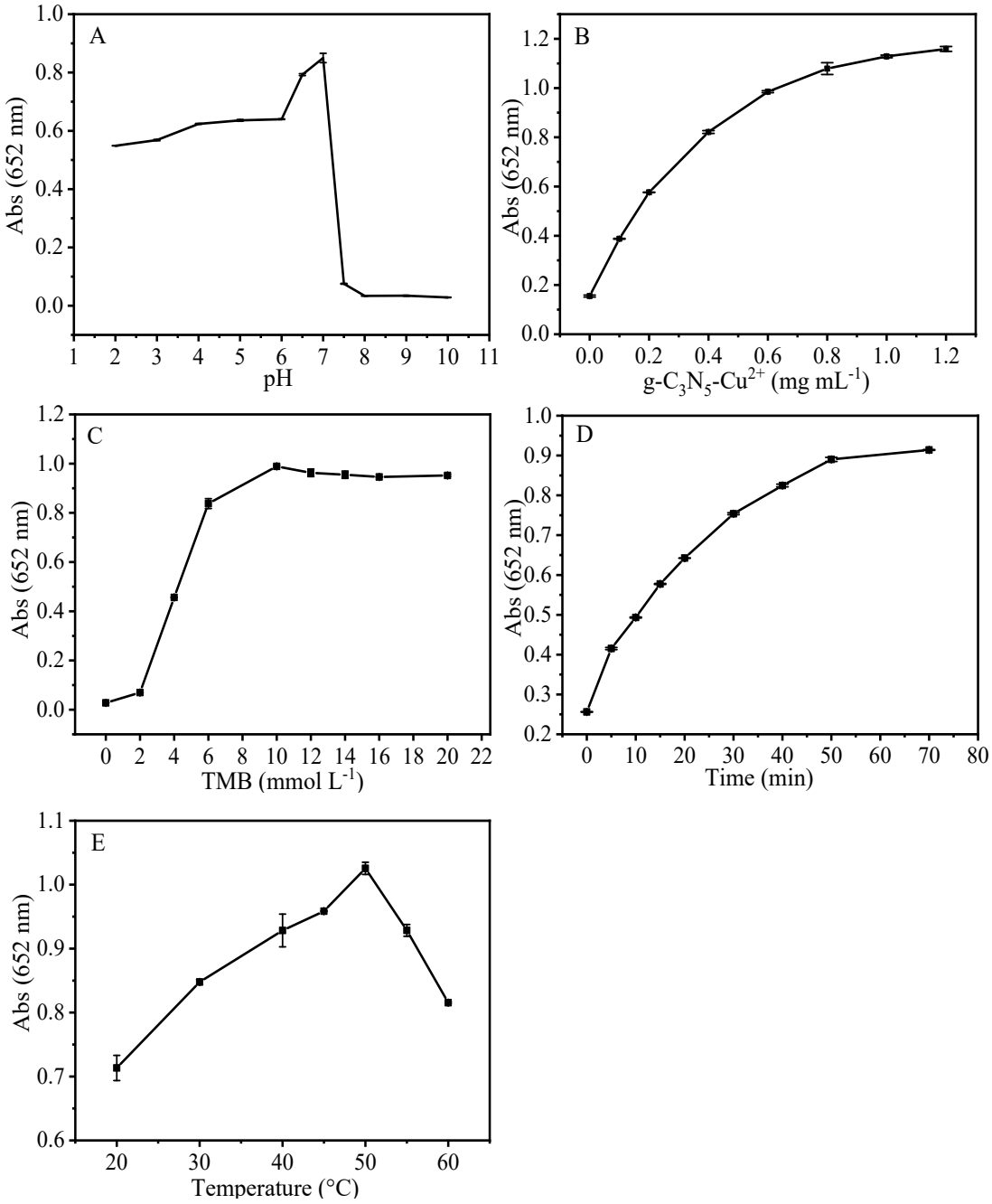

Figure S6. Effect of buffer pH (A), g-C_3N_5-Cu^{2+} NSs concentration (B), TMB concentration (C), reaction time (D), temperature (E), on the absorbance (at 652 nm) for the detection of H_2O_2.

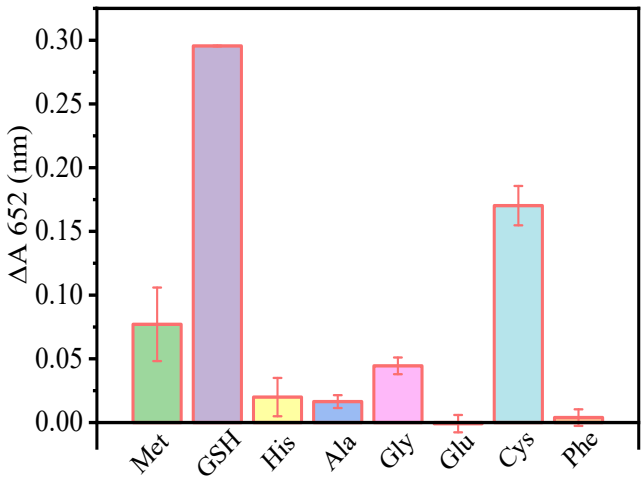

Figure S7. The absorbance of the mixed solution of g-C_3N_5-Cu^{2+} NSs, TMB and H_2O_2 on addition of 167 μmol L^{-1} Met, 167 μmol L^{-1} His, 167 μmol L^{-1} Ala, 167 μmol L^{-1} Gly, 167 μmol L^{-1} Glu, 16.7 μmol L^{-1} Cys, 167 μmol L^{-1} Phe and 16.7 μmol L^{-1} GSH, respectively.

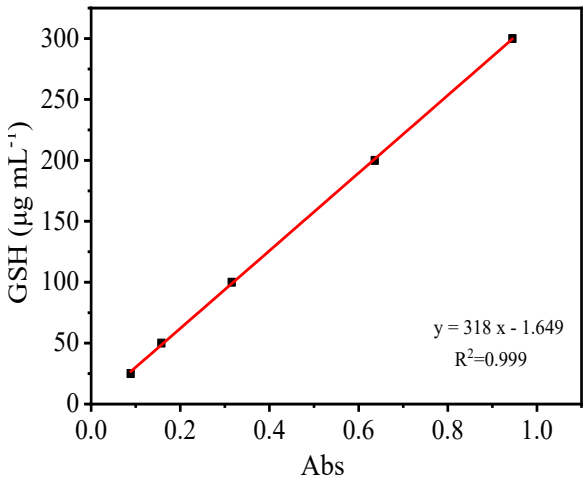

Figure S8. The linear calibration plot for GSH by commercial assay kit.

Table S1. Comparison of the kinetic parameters of g-C_3N_5-Cu^{2+} NSs, HRP and other peroxidase mimetics.

Catalyst	Substrate	K_m (mmol L^{-1})	V_{max} (mol L^{-1} s)	Ref
g-C_3N_5-Cu^{2+}	H_2O_2	1.0	1.8×10^{-6}	This work
	TMB	0.45	6.0×10^{-8}	
HRP	H_2O_2	10.9	58.5×10^{-8}	[S1]
	TMB	0.172	41.8×10^{-8}	
AuNPs@g-C_3N_4	H_2O_2	12.3	9.0×10^{-8}	[S2]
	TMB	0.097	1.52×10^{-8}	
Au-Ni/g-C_3N_4	H_2O_2	4.47	6.16×10^{-8}	[S3]
	TMB	0.16	2.34×10^{-8}	
g-C_3N_4-Cu NFs	H_2O_2	0.50	7.07×10^{-8}	[S4]
	TMB	0.53	16.6×10^{-8}	

Table S2. Comparison of peroxidase mimetics-based colorimetric methods for the detection of GSH.

Catalyst	Range	LOD	Ref
g-C_3N_5-Cu^{2+} NSs	0.83-33.3 μmol L^{-1}	0.25 μmol L^{-1}	This work
FeS_2 nanoparticles	0.2-0.35 μmol L^{-1}	0.15 μmol L^{-1}	[S5]
carbon nanodots	0-7 μmol L^{-1}	0.3 μmol L^{-1}	[S6]
CuS-polydopamine-Au composite	0.5-100 μmol L^{-1}	0.42 μmol L^{-1}	[S7]
Fe-Ne-C single atom nanozymes	100-400 μmol L^{-1}	78.33 μmol L^{-1}	[S8]
carbon nanoparticles	2.5-50 μmol L^{-1}	0.26 μmol L^{-1}	[S9]

Table S3. Detection of cellular GSH concentration.

Assay kit (μmol L^{-1})	Colorimetric method	Relative error (%)	Added (μmol L^{-1})	Found* (mean ± SD) (μmol L^{-1})	Recovery (%)	RSD (%)
12.9	11.4	-11.6	5.0	16.9 ± 0.1	103.0	0.6
			9.0	21.0 ± 0.4	101.9	1.9
			13.0	24.7 ± 0.5	100.4	2.1

*n=3

Reference

[S1] X. Meng, H. Zhao, M. Sun, Y. Zhang, Y. Zhang, X. Lv, H. Kim, M. Vainshtein, S. Wang, G. Qiu, *Sci. Total Environ.* 2019, **675** 213-223.

[S2] N. Wu, Y. Wang, X. Wang, F. Guo, H. Wen, T. Yang, J. Wang, *Anal. Chim. Acta* 2019, **109**, 69-75.

[S3] G. Darabdhara, J. Bordoloi, P. Manna, M. Das,, *Sensors and Actuat. B* 2019, *285,* 277-290.

[S4] T. Dang, N. Heo, H. Cho, S. Lee, M. Song, H. Kim, M. Kim, *Microchim. Acta,* 2021, **188**, 293.

[S5] C. Song, W. Ding, W. Zhao, H. Liu, J. Wang, Y. Yao, C. Yao, *Biosens. Bioelectron*. 2020, *151*, 111983.

[S6] M. Shamsipur, A. Safavi, Z. Mohammadpour, *Sensor Actuat. B-chem*. 2014, **199**, 463-469.

[S7] Y. Wang, Y. Liu, F. Ding, X. Zhu, L. Yang, P. Zou, H. Rao, Q. Zhao, X. Wang, *Anal. Bioanal. Chem.* 2018, **410**, 4805-4813.

[S8] W. Lu, S. Chen, H. Zhang, J. Qiu, X. Liu, *J. Materiomics* 2022, **23**, 52-8478.

[S9] L. Chen, X. Li, Z. Li, K. Liu, J. Xie, *RSC Adv.* 2022, **12**, 595-601.